Indian J. Met. Hydrol. Geophys. (1978), **29**, 1 & 2, pp. 375-383

551.553.21 : 551.509.313 : 551.558.21

The inclusion of Himalayas in a primitive equation model

P. K. DAS and H. S. BEDI

Meteorological Office, New Delhi

ABSTRACT. A regional primitive equation model has been developed for the Indian region. One of the difficulties in this model is caused by large gradients in mountainous regions. To avoid large truncation errors near the edges of mountains, some models evaluated the pressure gradient force on a constant pressure surface, instead of a sigma surface. More recently, phillips (1974) suggested that truncation errors could be reduced by removing the hydrostatic component of the geopotential field. The residual geopotential may then be treated as a dependent variable, which could be integrated with respect to time by the model. To be energetically consistent, a temperature field was similarly defined. This paper discusses the scheme for the Himalayan region. Truncation errors by the present scheme are compared with the earlier method. The conversion from sigma to pressure coordinates was carried out by Lagrangian interpolation. Results are presented with these methods to show the development of circulations in 5 days of model time.

1. Introduction

In an earlier study, Das and Bedi (1976) examined the influence of the Himalayas on idealized zonal flow. Starting with different zonal profiles, the model was integrated upto 3 days. This revealed interesting patterns, such as, (*a*) the formation of a deep trough to the east of the Himalayas, (*b*) anticyclonic curvature of streamlines induced by the Western Ghats and (*c*) an area of low pressure, resembling the monsoon trough, if the initial zonal profile had meridional and vertical shear. But, the model also revealed serious limitations. Large truncation errors developed in the vicinity of the mountains, and the change over from sigma to pressure coordinates gave rise to an unrealistic anticyclone over India. The purpose of the present paper is to discuss a method due to Phillips (1974) for overcoming truncation errors. We also present results which were obtained by Lagrange's interpolation for conversion from sigma to pressure coordinates. Lastly, results are presented for 5 days of model time, instead of 3 days, with two initial wind profiles. One had no shear, while the other had meridional and vertical shear.

2. Description of the model

The model was a modified version of the one developed by Shuman and Hovermale (1968). The horizontal and vertical resolution was limited to some extent by the constraints of computer memory. The rectangular domain of the model extended from the equator to 60°N, and from 0° to 140°E. In the vertical, the atmosphere was divided into three layers of equal thickness. Sigma coordinates were used to measure vertical depth. Its advantage was to simplify the lower and upper boundary conditions. The input data consist of geopotentials for 850, 700, 500, 300 and 200 mb along with sea level pressure. The unit grid was 250 km, and variations in the map factor were neglected for simplicity.

The basic equations of the model are :

$$u_t + (uu_x + vu_y + \dot{\sigma}u_\sigma) - fv = -\phi_x - c_p\theta\pi_x + \mu\nabla^2 u \qquad (2.1)$$

$$v_t + (uv_x + vv_y + \dot{\sigma}v_\sigma) + fu = -\phi_y - c_p\,\theta\pi_y + \mu\nabla^2 v \qquad (2.2)$$

$$\phi_\sigma + c_p\,\theta\pi_\sigma = 0 \qquad (2.3)$$

$$\theta_t + (u\theta_x + v\theta_y) + \dot{\sigma}\,\theta_\sigma = 0 \qquad (2.4)$$

$$p_{\sigma t} + (up_\sigma)_x + (vp_\sigma)_y + (\dot{\sigma}p_\sigma)_\sigma = 0 \quad (2.5)$$

On differentiating (2.5) we have,

$$p_\sigma \dot{\sigma}_\sigma + p_\sigma(u_{\sigma x} + v_{\sigma y}) + (u_\sigma p_{\sigma x} + v_\sigma p_{\sigma y}) = 0 \quad (2.6)$$

$$\sigma = \frac{p - 200}{p_s - 200} \text{ and } \pi = \left(\frac{p}{1000}\right)^\kappa \quad (2.7)$$

The symbols are :

u, v : the zonal and meridional components of wind in cartersian coordinates (0 x, 0 y), where the x and y axes measure distances to the east and north respectively

p : pressure

ϕ : geopotential

θ : potential temperature

c_p : specific heat at constant pressure

μ : diffusion coefficient ($10^5 m^2 sec^{-1}$)

κ : R/c_p

The Himalayas were represented by an elliptic block

$$H(x, y) = H_0\left[1 - \left(\frac{x^2}{a^2} + \frac{y^2}{b^2}\right)\right] \quad (2.8)$$

The maximum height of the block (H_0) was 5 km, while a and b were set at 1750 and 1000 km respectively in the zonal and meridional directions. The centre of the block was placed at 35°N, 91·3°E. For the Western Ghats and the Burma mountains, smoothed profiles were derived from appropriate maps. The topographic features are shown in Fig. 1.

A non-staggered horizontal grid, with the averaging and differencing scheme of Shuman and Hovermale (1968), was used (Bedi and Das 1975). This scheme, though not strictly energy conserving, was satisfactory for short range predictions. For boundary conditions, the vertical velocity ($\dot{\sigma}$) was made to vanish at the top and bottom of the model atmosphere. Along the lateral walls, the time derivatives of all dependent variables vanished. We put,

$$\left.\begin{aligned} u_t = v_t = 0 \\ p_{\sigma t} = \theta_t = 0 \end{aligned}\right\} \text{ at } \begin{aligned} x &= 0 \text{ and } L \\ y &= 0 \text{ and } L \end{aligned} \quad (2.9)$$

3. Reduction of truncation errors

The two terms on the right of equations (2·1) and (2·2) represent forces due to pressure gradient. They acquire very large values near steep mountain slopes, and nearly balance each other. It is customary to reduce truncation errors by evaluating pressure gradients on a surface of constant pressure, rather than on a sigma surface (Kurihara 1968). An alternative approach was suggested by Phillips (1974). This seeks to remove the hydrostatic component of the geopotential field, and to subsequently consider the residual geopotential as a dependent variable. As the variables thus involved are now substantially reduced, even in the vicinity of mountains, the gradients are also decreased to a large extent.

We define

$$\begin{aligned} \phi'(x, y, p, t) &= \phi(x, y, p, t) - \bar{\phi}(p) \\ \theta'(x, y, p, t) &= \theta(x, y, p, t) - \bar{\theta} \end{aligned} \quad (3.1)$$

where $\bar{\phi}(p)$ is the mean geopotential of a surface of constant pressure (p). A mean potential temperature for the region is defined by

$$\bar{\theta} = [< \phi_T > - < \phi_S >] \div [c_p (< \pi_s > - \pi_T)] \quad (3.2)$$

The subscripts T and S refer to the upper and lower boundaries, and $< >$ denotes an average value. Thus, $<\phi_s>$ is the mean surface geopotential and

$$\bar{\phi}(p) = [< \phi_S > (\pi - \pi_T) - < \phi_T >) \times (< \pi_S > - \pi] \div [< \pi_S > - \pi_T] \quad (3.3)$$

Introducing (3.2), (3.3) on the right hand side of (2.1), (2.2) we have

$$\nabla_\sigma \phi - c_p \theta \nabla_\sigma \pi = \nabla_\sigma \phi' - c_p \theta' \nabla_\sigma \pi \quad (3.4)$$

From contours of the topographic features, we computed the sea level pressure (p_S) by assuming hydrostatic balance. Thus,

$$\phi_S - \phi_0 = RT_S \ln(p_S/p_0) \quad (3.5)$$

where $p_0 = 1000$ mb and T_S is a mean temperature between sea level and the height of the barrier. The deviations (ϕ') from the mean geopotential field were then computed by (3.1) for different constant pressure surfaces. Subsequently, the appropriate value of ϕ' for a given sigma surface was obtained by Lagrange's interpolation. This seeks to derive a polynomial for ϕ' of the form

$$(\phi')_\sigma = \sum_{K=1}^{5} L_K(p)(\phi')_K \quad (3.6)$$

where the index K refers to value of ϕ' on different standard pressure surfaces, and $L_K(p)$ is

$$L_K(p) = \frac{(p - p_S)(p - 850)\ldots\ldots(p - 200)}{(p_K - p_S)(p_K - 850)\ldots(p_K - 200)} \quad (3.7)$$

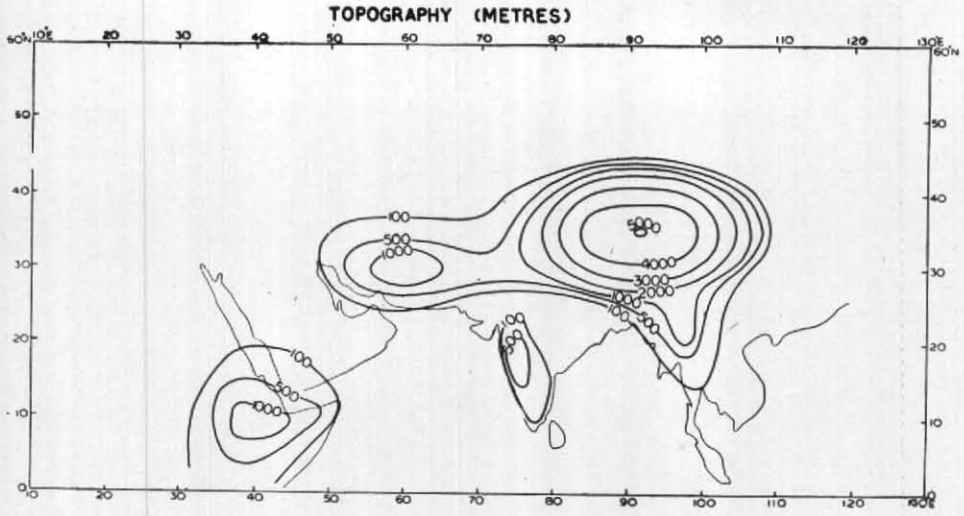

Fig. 1. Surface topography

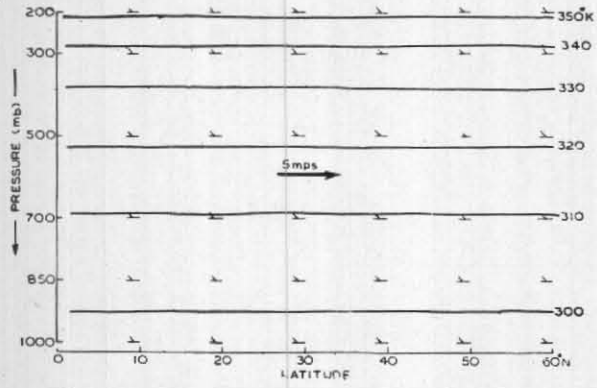

Fig. 2 (a). Initial temperature and wind profile (no shear)

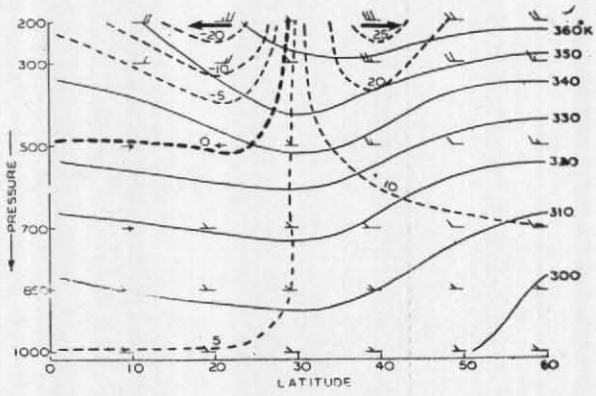

Fig, 2 (b). Initial temperature and wind profile (with shear)

It was observed that the use of (3·4), together with (3·6) and (3·7) considerably reduced truncation errors. If, as in our previous work, the appropriate value of ϕ on a sigma surface was obtained by hydrostatic interpolation between two adjacent pressure surfaces, we found that unrealistic high pressures were generated at all pressure levels. We observed, for example, that at 300 mb the geopotential at any grid point above the mountain was higher by as much as 80 geopotential metres, when compared with values at adjoining grid points. This happened immediately after initialization. The result of this was to create an unrealistic high pressure area over the mountain. But, if the hydrostatic component of the geopotential field was first removed, as indicated by (3·1), (3·2) and (3·3), and Lagrangian interpolation was used, then the geopotential values over the mountain and over the plains did not differ by more than 20 geopotential metres. This corresponds to an error of less than 1°C in temperature at 300 mb. At lower levels, the errors were considerably less than 20 geopotential metres. We were thus led to infer that large truncation errors, and errors caused by faulty interpolation, could be reduced by a combination of the algorithm of Phillips (1964) and Lagrangian interpolation.

4. Initialization and integration procedure

Two wind profiles were used in the experiment. One had no shear, while the second had zonal and meridional shear. The temperature and geopotential fields, which were compatible with these profiles,

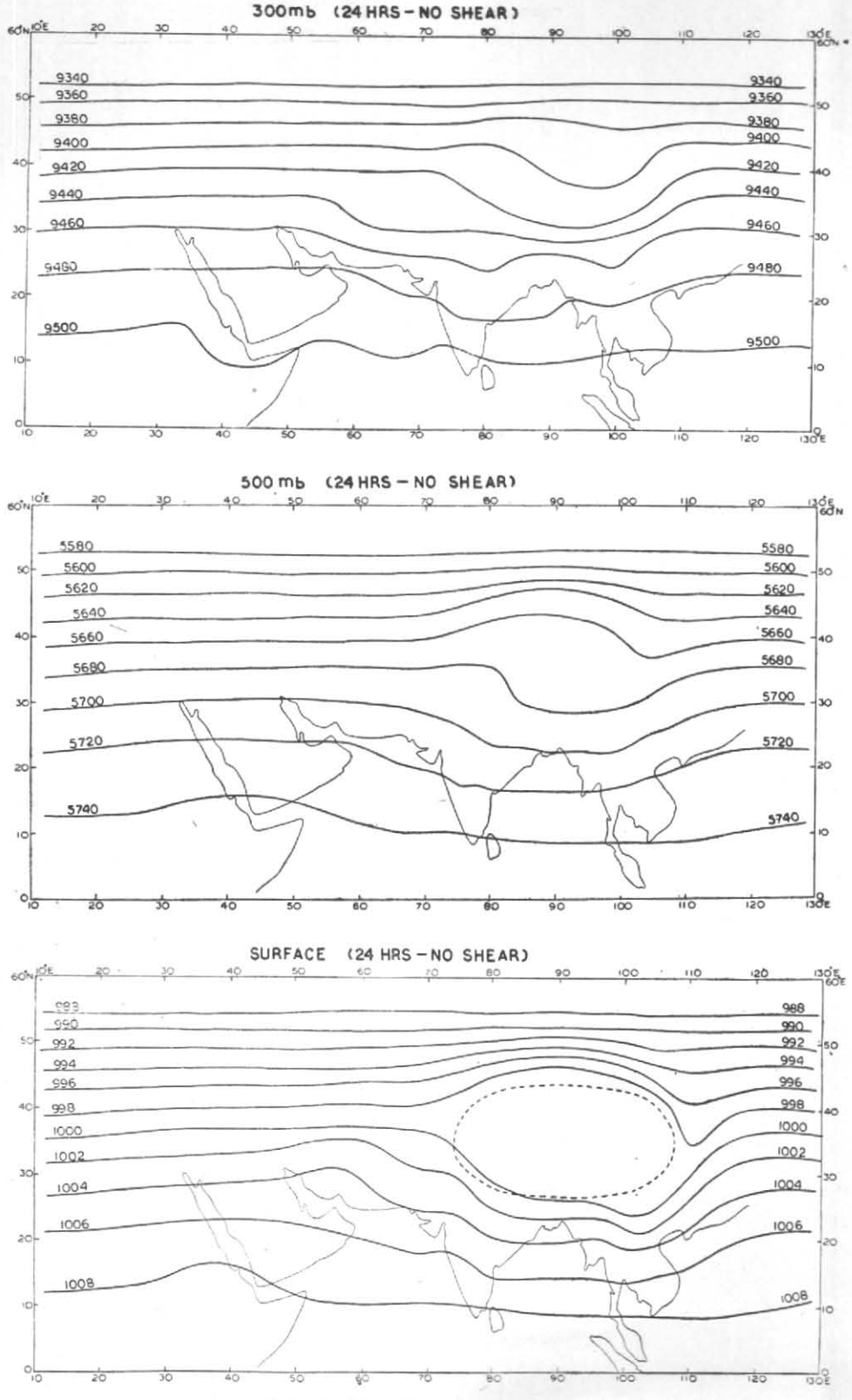

Fig. 3 (a) Results of integration for initial wind profile with no shear (24 hr)

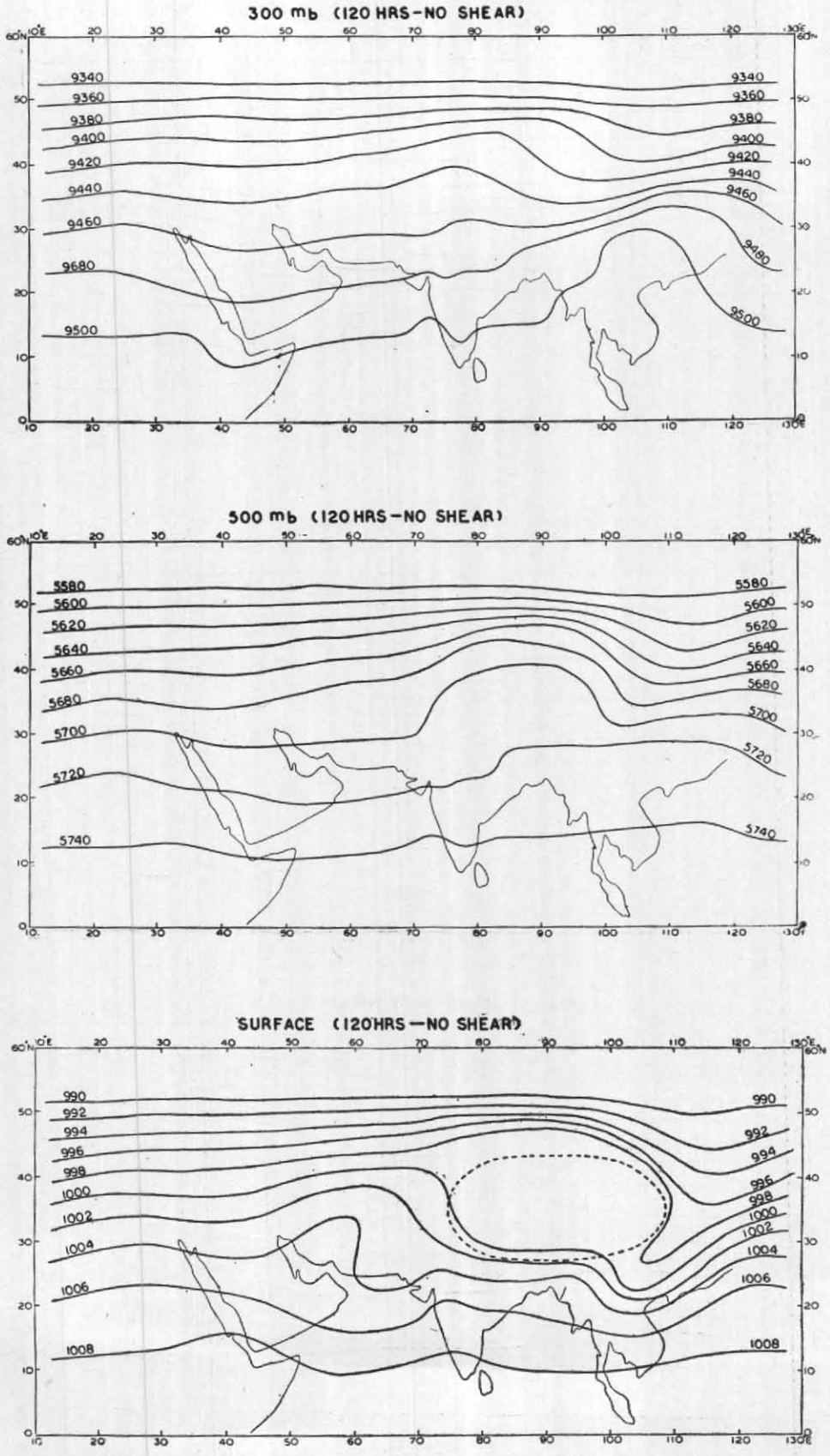

Fig. 3 (b). Results of integration for initial wind profile with no shear (120 hr)

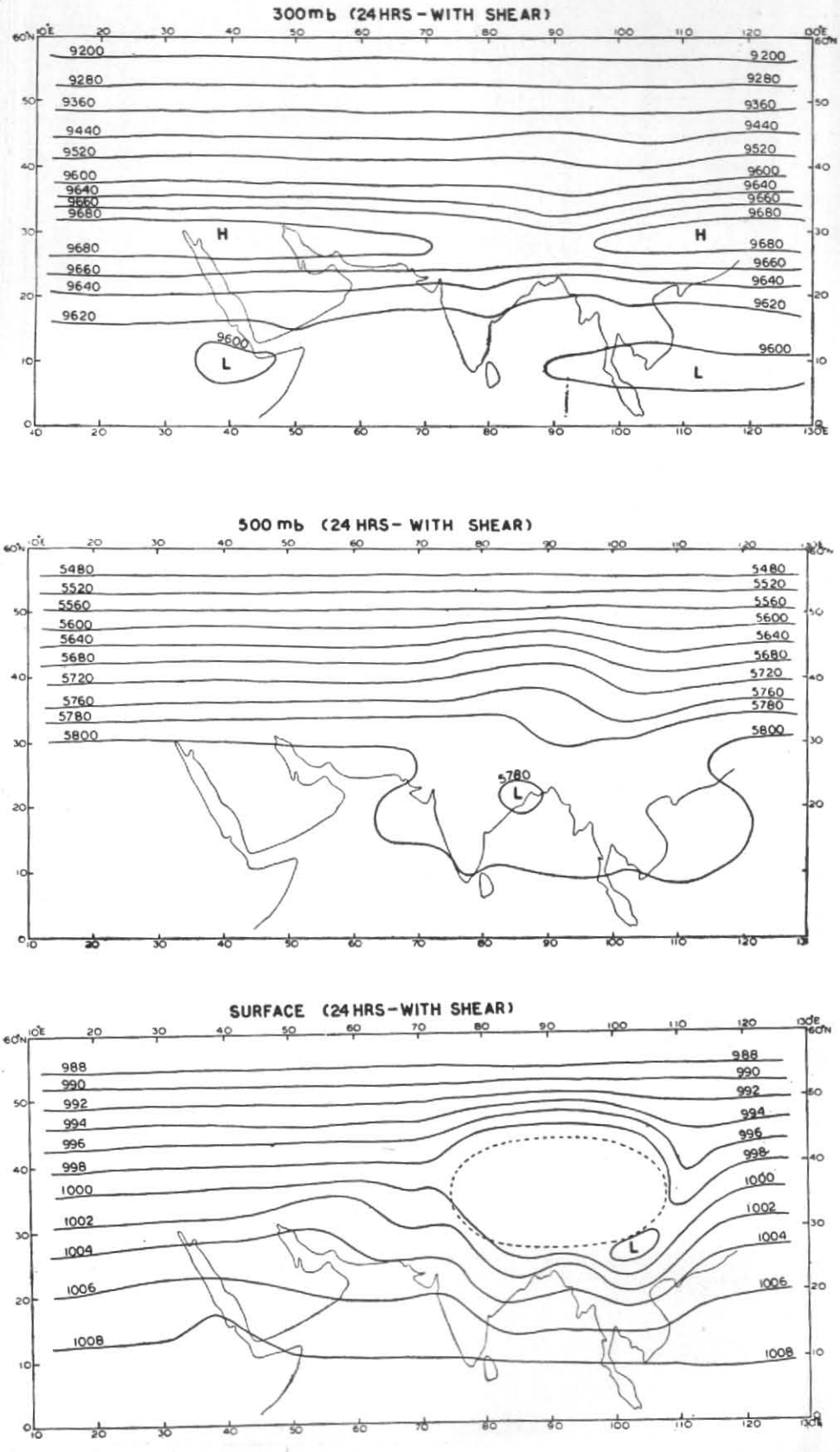

Fig. 4 (a). Results of integration for initial wind profile with shear (24 hr)

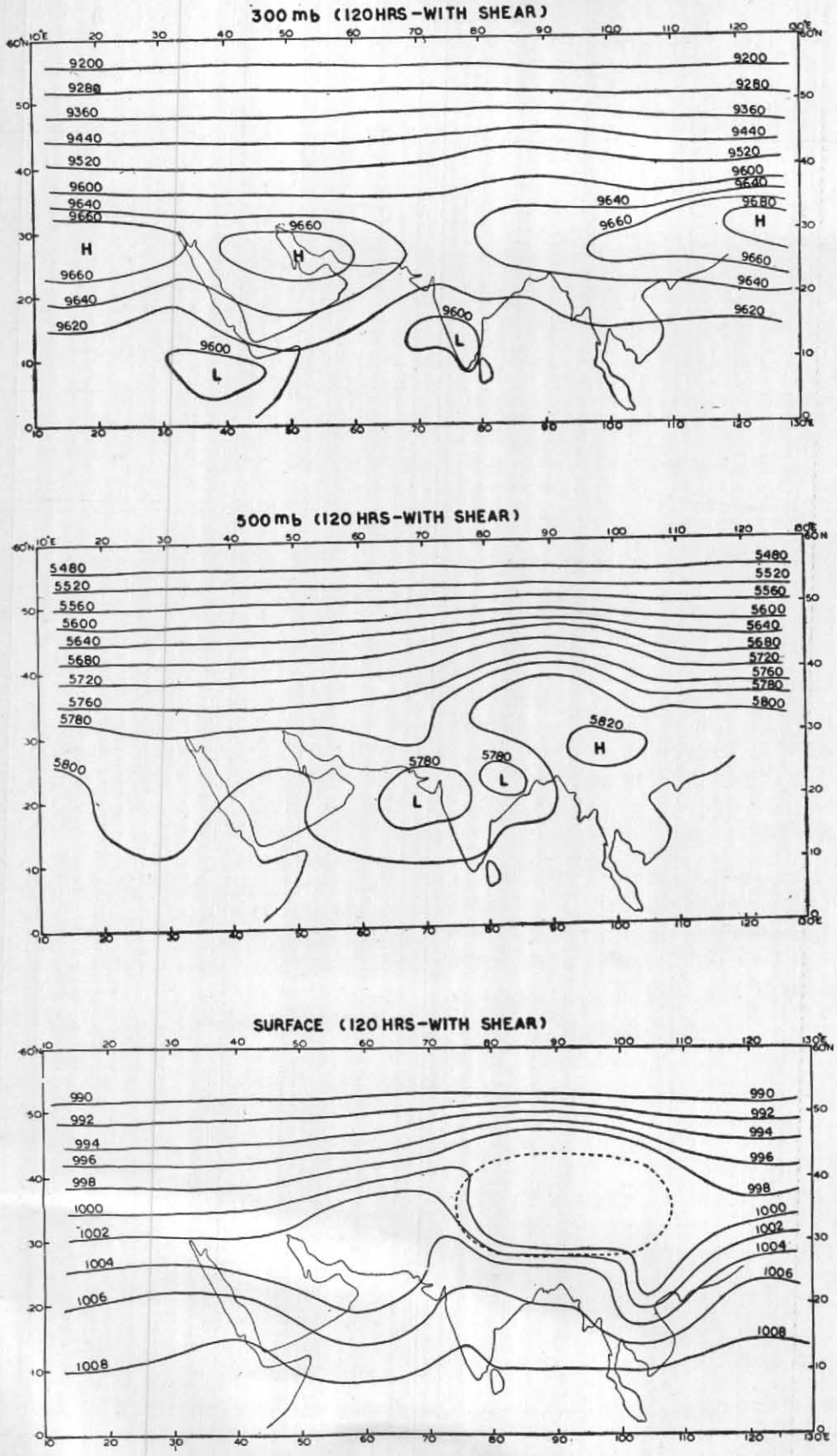

Fig. 4 (b). Results of integration for initial wind profile with shear (120 hr)

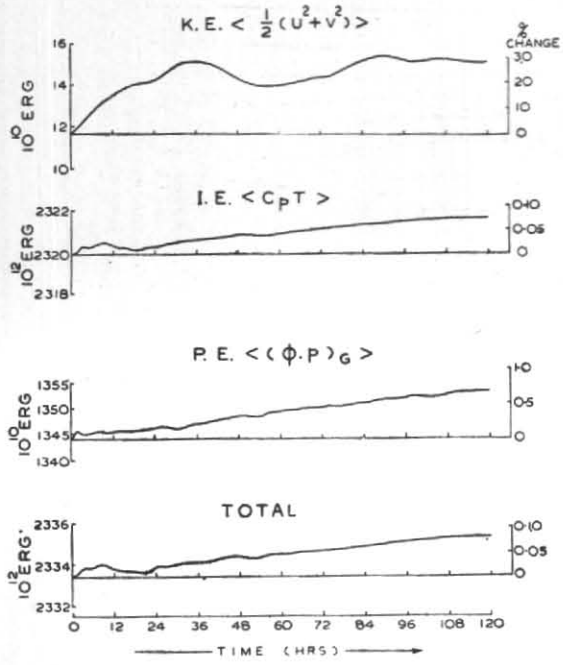

Fig. 5 (a). Time variation of energy for profile with no shear

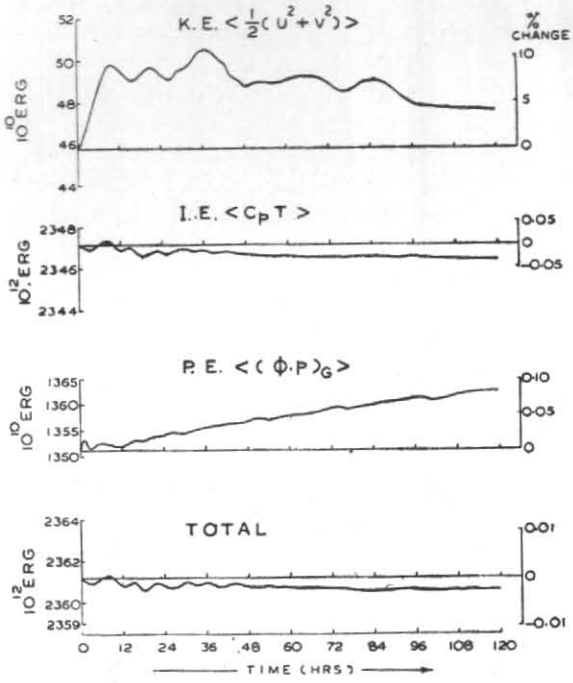

Fig. 5 (b). Time variation of energy for profile with shear

were derived with the help of the geostrophic and thermal winds. The second profile was consistent with the actual observed temperature and wind during the month of July along the 80° meridian. These initial profiles are shown in Fig. 2.

The integration was carried upto 5 days with a semi-implicit scheme, and time step ($\triangle t$) of 10 min. A weak time-smoother was used during the integration. Thus, a dependent variable (A^*) was smoothed at time n by

$$\bar{A}\,(n) = A^*(n) + 0.01[\bar{A}(n-1) - 2A^*(n) + A^*(n+1)] \quad (4.1)$$

After every 24 hours, a similar smoothing was done on the space variables.

A scheme for dynamic initialization was used. This involved three cycles of forward integration of the model for 1 hour followed by backward integration for another hour. One half the initial pressure and height fields were restored at the end of each cycle, while the wind field was allowed to adjust freely. The diffusion terms were not included during the course of initialization.

It was observed that the model could be run upto 36 hours of model time without difficulty; but beyond this period the process of initialization had to be repeated. This difficulty was partly caused by the reflective boundary conditions that were used at the lateral walls of the region. It appeared, that the gravitational modes of motion excited by the mountains were prevented from being dispersed by these boundary conditions; consequently, they had to be damped by initialization once every 24 hours. This aspect of the present study is being further investigated and will be reported in a subsequent paper. In Fig. 5 we show the variation of different forms of energy with time. The kinetic energy showed a sharp increase upto about 36 hours of integration for both wind profiles. Thereafter, the kinetic energy showed relatively small variations with a decreasing tenddency for the wind profile with shear. The variation of potential energy showed a slight increase with time. In Fig. 5 we have also shown the variation of total energy with time, which shows a slight increase for profile with no shear, and a slight decrease for a profile with shear. The total change during 5 days was, however, within 0·1 per cent for both the cases. It is difficult to see how these energy changes are brought about, unless more is known about the respective roles of (*a*) the rotational modes and (*b*) the gravitational modes that are generated by the mountains. As we are dealing with a non-linear baroclinic system,

interactions between different waves could be also important.

As in the earlier study, integration upto 5 days with a wind profile without shear brought out lee troughs to the east of the Himalayas, the Western Ghats and the Burma mountains. At the end of 120 hours these troughs showed some intensification and a movement eastward by 10-15° longitude. There was no indication of the development of a monsoon trough with a purely zonal profile. These developments are shown in Fig. 3.

For a wind profile with meridional and vertical shear, similar lee troughs were observed (Fig. 4). But, in this case, a low pressure area developed over the Gangetic plains resembling a monsoon trough at 500 mb. It was interesting to see that the mechanical effect of the mountains was capable of generating a low pressure area of this nature, but it was not clear why the low pressure zone built up at 500 mb instead of lower levels. At the end of 120 hours, the troughs to the lee of the Western Ghats and the Burma mountains did not show much change, but the trough to the east of the Himalayas moved eastwards by about 20° longitude upto 700 mb.

An interesting feature was the development of a ridge at 300 mb. At the end of 120 hours, the ridge at 300 mb had become very well marked, and looked very similar to the subtropical ridge observed over India. An examination of temperature changes showed considerable advection of cold air from regions to the north of the mountains. It appears plausible to assume that the anticyclonic circulation, which is a common feature of the monsoon circulation in the upper troposphere, is a result of cold air advection. The advection is generated by the presence of the Himalayan barrier.

5. Summary and conclusions

The main results of this study may be summarized as follows :

(*i*) We observed considerable reduction in (*a*) truncation errors, and (*b*) errors in conversion from pressure to sigma surfaces by removing the hydrostatic component of the geopotential and by using Lagrange's interpolation formula.

(*ii*) Extended integration of the model upto 5 days required initialization every 24 hours. This suggests that gravitational modes, generated by mountains, were not being dispersed adequately. Partly this could be a consequence of reflective boundary conditions on the lateral walls.

(*iii*) Initial zonal flow with shear generated a low pressure area, resembling a monsoon trough, at 500 mb. This was not observed if the initial flow had no shear.

(*iv*) Anticyclonic circulation, resembling the subtropical ridge was generated at 300 mb after 120 hours. This was associated with advection of cold air from the north of the Himalayas.

REFERENCES

Das, P. K. and Bedi, H. S.	1976	A study on orographic effects by a primitive equation model. Proc. of the IITM Symp. on "Tropical Monsoons" held in Pune, India, September 1976, pp. 51-58.
Kurihara, Y.	1968	*Mon. Weath. Rev.*, **96**, pp. 654-656.
Phillips, M. A.	1974	*Tech. Note*, 104, N.M.C. Washington. pp. 40.
Shuman, F. G. and Hovermale, J. B.	1968	*J. appl. Met.*, **7**, pp. 525-547.